



**Environmental  
Science**  
Processes & Impacts

**Aqueous processing of water-soluble organic compounds in  
the eastern United States during winter**

Journal:	<i>Environmental Science: Processes &amp; Impacts</i>
Manuscript ID	EM-ART-03-2022-000115.R1
Article Type:	Paper

SCHOLARONE™  
Manuscripts

## Environmental Significance Statement

Water-soluble organic compounds (WSOC<sub>p</sub>) make up a significant contribution towards the total organic mass in the atmosphere. These compounds are likely to have impacts on human health and climate. Thus, the characterization of the pathways responsible for the formation of these compounds is essential in understanding such impacts. In this work, we provide evidence for the formation of water-soluble species through absorptive partitioning and aqueous processing. We highlight that water mediates WSOC<sub>p</sub> formation through aqueous processing under specific temperature conditions. We demonstrate that particle drying does not induce any primary nor secondary WSOC<sub>p</sub> evaporation in the winter. Analyses show that aqueous WSOC<sub>p</sub> in the winter is controlled by the presence of sufficient amounts of, the temperature-dependent, aerosol water and biomass burning precursors.

# Aqueous processing of water-soluble organic compounds in the eastern United States during winter

Marwa M. H. El-Sayed<sup>1,†</sup>, Christopher J. Hennigan<sup>2</sup>

<sup>1</sup>Department of Civil Engineering, Embry-Riddle Aeronautical University, Daytona Beach, FL USA.

<sup>2</sup>Department of Chemical, Biochemical and Environmental Engineering, University of Maryland, Baltimore County, Baltimore, MD, USA.

†Corresponding author: M.M.H. El-Sayed ([elsayedm@erau.edu](mailto:elsayedm@erau.edu))

## Abstract

Aqueous multi-phase processes are significant contributors to organic aerosol (OA) mass in the atmosphere. This study characterizes the formation of water-soluble organic matter during the winter in the eastern United States through simultaneous measurements of water-soluble organic carbon in the gas and particle phases (WSOC<sub>g</sub> and WSOC<sub>p</sub>, respectively). The formation of secondary WSOC<sub>p</sub> occurred primarily through two pathways: (1) absorptive partitioning of oxygenated organics to the bulk OA and (2) aqueous phase processes. WSOC<sub>p</sub> formation through the former pathway was evident through the relationship between the fraction of total WSOC in the particle phase ( $F_p$ ) and the total OA concentration. Conversely, evidence for nighttime aqueous WSOC<sub>p</sub> formation was based upon the strong enhancement in  $F_p$  with increasing relative humidity, indicating the uptake of WSOC<sub>g</sub> to aerosol liquid water (ALW). The  $F_p$ -RH relationship was only observed for temperatures between 0 – 10 °C, suggesting conditions for aqueous multi-phase processes were enhanced during these times. Temperature exhibited an inverse relationship with ALW and a proportional relationship with aerosol potassium. ALW and biomass burning precursors were both abundant in the 0 – 10 °C temperature range, facilitating aqueous WSOC<sub>p</sub> formation. To assess the impact of particle drying on the WSOC<sub>p</sub> concentrations, the particle measurements alternated between ambient and dried channels. No change was observed in the concentration of particles before and after drying, indicating that the WSOC<sub>p</sub> formed through the uptake of WSOC<sub>g</sub> into OA and ALW remained in the condensed phase upon particle drying at all temperature ranges. This work contributes to our understanding of sources, pathways, and factors affecting aqueous aerosol formation in the winter.

## 1 Introduction

Water-soluble organic carbon (WSOC<sub>p</sub>) represents an important component of fine organic aerosol (OA) in the atmosphere<sup>1-4</sup>. WSOC<sub>p</sub>, collectively made up of thousands of individual compounds, has direct impacts on particle hygroscopicity<sup>5-6</sup>, light absorption<sup>7</sup> and thereby on the climate system. Further, these species may have profound impacts on human health<sup>8</sup>. WSOC<sub>p</sub> has two predominant sources in the atmosphere: it is emitted directly from biomass burning<sup>9-13</sup>, and it is formed through secondary processes from many VOC precursors<sup>2,14-16</sup>.

A prominent pathway for secondary WSOC<sub>p</sub> formation is the uptake and reaction of water-soluble VOCs in atmospheric aerosol liquid water (ALW)<sup>17-18</sup>. Because WSOC<sub>p</sub> often represents a large fraction of total OA mass (typically 30 – 80%), such aqueous processes also contribute significantly to secondary OA (SOA), as well. While the abundance of water-soluble gaseous precursors is key in the aqueous processing of atmospheric particles, ALW is also a critical

parameter in this process<sup>1</sup>. The initial uptake of water-soluble gases into ALW is an equilibrium process<sup>19</sup>, suggesting that any evaporation of ALW will shift this equilibrium and might consequently lead to a loss in condensed-phase organics back to the gas phase<sup>18</sup>. Particle drying is a natural phenomenon that occurs in the atmosphere due to changes in relative humidity (RH) throughout the day and through changes in RH that accompany vertical atmospheric transport. In previous work conducted by our group, we reported a seasonal dependence of OA evaporation induced by particle drying. During the summer, we observed significant WSOC<sub>p</sub> evaporation due to particle drying, which was attributed to reversible aqSOA formation U.S.<sup>18</sup>. This was not observed in other seasons, except for the late spring<sup>20</sup>.

During winter, biomass burning – especially that produced from residential heating – represents an important OA source in many locations<sup>21-22</sup>. Studies show that water-soluble organics in the particle phase make up almost 40% of wood-burning emissions (e.g.,<sup>23</sup>) and that more than 50% of biomass-burning OA is water soluble (e.g.,<sup>12</sup>). Biomass burning emissions include an array of water-soluble gases that may contribute to WSOC<sub>p</sub> such as phenols<sup>24</sup>. In the eastern U.S., biomass burning is a significant contributor to WSOC<sub>p</sub> concentrations in the winter<sup>25</sup>. Biomass burning emits various VOCs, hence, secondary OA formation may be substantial<sup>26-27</sup>. Further, significant amounts of primary OA are also emitted, many of which are semi-volatile and could ultimately lead to further processing of OA<sup>28</sup>. Laboratory studies provide evidence for dynamic transformations of numerous compounds emitted from biomass combustion and significant potential to form aqueous WSOC<sub>p</sub><sup>24,29-35</sup>. Field and modeling studies demonstrate secondary OA formation in the aqueous phase from biomass burning in diverse locations that include Fresno, U.S.<sup>36</sup>, Paris, France<sup>37</sup>, Douai, northern France<sup>38</sup>, Los Angeles, U.S.<sup>39</sup>, the Po Valley, Italy<sup>40</sup>, and China<sup>41-44</sup>.

SOA formation has been studied more intensely during summer than winter because the summertime corresponds to a peak in biogenic VOC emissions and enhanced photochemical activity in many locations. For example, SOA chamber studies utilize lower tropospheric summertime temperatures far more frequently than winter temperatures<sup>45</sup>. Further, large-scale intensive field campaigns investigating SOA formation in the U.S. have historically been more frequent in the summer than in the winter<sup>46</sup>. Similarly, studies of WSOC<sub>p</sub> formation have also been less frequent during winter (e.g.,<sup>2,15,18,47-52</sup>), especially those investigating secondary aqueous pathways<sup>18</sup>. Studies of this type have been frequently conducted in China, due to the severe winter haze episodes that affect air quality in many cities<sup>42-44</sup>. Significant differences exist in the fuels used for residential heating between the U.S. and China. In the U.S., residential heating relies mainly on wood burning whereas in China, coal burning is used extensively for heating purposes<sup>53</sup>. This suggests there may also be key differences in the WSOC<sub>p</sub> mass and its formation pathways in the U.S. during winter.

The purpose of this work is to characterize WSOC<sub>p</sub> formation and its potential sources in Baltimore, Maryland during the winter. We also characterize the effect of particle drying on primary and secondary WSOC<sub>p</sub>, including that formed through aqueous processes. Baltimore is located in the highly populated and heavily trafficked Mid-Atlantic region of the U.S. It is strongly influenced by emissions from industrial activities and major interstate routes<sup>52</sup>. Biomass burning contributes approximately 17% to wintertime PM<sub>2.5</sub> mass concentrations in the region, as well<sup>54</sup>. Isoprene emissions dominate the VOC budget in the region during summertime but are very low during winter<sup>55</sup>. Thus, this study contrasts prior results by investigating the formation of aqueous organic aerosol through secondary and irreversible processes from biomass burning for residential heating.

## 2 Materials and Methods

### 2.1 Measurement location

Ambient measurements were conducted at a suburban location (39.2546° N, -76.7094° W) on the campus of the University of Maryland, Baltimore County (UMBC). A suite of instrumentation was placed on the rooftop of the UMBC Engineering Building, approximately 20 – 25 m above ground level. UMBC is almost 10 km from downtown Baltimore, about 10 km from Baltimore – Washington International Airport (BWI) and approximately 60 km from Washington, D.C. Wintertime measurements were carried out from 4 to 21 February and from 6 to 23 March, 2015. This sampling period included a wide range of meteorological conditions (Table 1) and source influences.

### 2.2 Water-soluble organic carbon measurements

The measurements presented in this work have been described in detail elsewhere<sup>18,20,55</sup>. Briefly, a Mist Chamber (MC)<sup>56</sup> and a Particle-Into-Liquid-Sampler (PILS)<sup>57-58</sup>, were used to sample WSOC<sub>g</sub> and WSOC<sub>p</sub>, respectively, and were both connected to a Total Organic Carbon Analyzer (TOC; model 900 Turbo, GE Analytical). The air sample passed through a 47 mm quartz fiber filter before it enters the MC to remove any particles in the sample. The air sample to the PILS was first passed through a parallel plate carbon denuder to remove interference from semi-volatile organic compounds. Dynamic blanks were measured every other day for the PILS and MC systems in the same way the sampling took place except that the vacuum pumps were turned off. Blanks were used to quantify the method limit of detection (LOD, which is calculated as three times the standard deviation of the blanks) for WSOC<sub>p</sub> (0.33 μg-C m<sup>-3</sup>) and WSOC<sub>g</sub> (0.43 μg-C m<sup>-3</sup>).

The characterization of the effect of particle drying on WSOC<sub>p</sub> concentrations was conducted by directing the WSOC<sub>p</sub> air sample through a silica gel diffusion dryer (WSOC<sub>p,dry</sub>) and comparing its concentration to the WSOC<sub>p</sub> measured in a parallel, unperturbed channel<sup>18,20,55</sup>. Total drying time in the silica drier was ~7 s. This amount of time far exceeds the required time for aerosol water evaporation, which is on the order of 10<sup>-3</sup> s for fine particles<sup>59</sup>. This drying time may not allow for complete evaporation of condensed organics but is sufficient to provide evidence of evaporation if it occurs. More detailed discussion about this point is provided in El-Sayed et al.<sup>55</sup>. Particle losses through the diffusion dryer were measured and were found to be minimal<sup>55</sup>. The dry channel was maintained at a relative humidity (RH) of ~20% while the ambient channel was maintained at ambient RH<sup>20</sup>. A WSOC<sub>p,dry</sub>/WSOC<sub>p</sub> ratio of unity implies that the WSOC<sub>p</sub> did not evaporate with drying<sup>55</sup> whereas a ratio less than unity occurs if particle drying results in some WSOC<sub>p</sub> evaporation<sup>18</sup>. A single cycle of WSOC<sub>p</sub> – WSOC<sub>p,dry</sub> – WSOC<sub>g</sub> measurements was completed every 14 minutes, which allowed for the characterization of dynamic changes in the factors influencing SOA formation during the winter. A total of 2440 WSOC<sub>p</sub> – WSOC<sub>p,dry</sub> – WSOC<sub>g</sub> measurement cycles were carried out for this study<sup>60</sup>.

### 2.3 Aerosol Liquid Water (ALW)

A climatology of wintertime ALW concentrations was derived based upon five years of aerosol composition measurements in Baltimore. Organic and inorganic concentrations of fine particulate matter (PM<sub>2.5</sub>) were provided by the Maryland Department of the Environment (MDE) at their HU-Beltsville site (AQS ID 240330030, approximately 25 km from UMBC

(latitude of 39.2557° N and longitude of 76.7110° W). Inorganic and OA concentrations on 24-h filters were measured by MDE once every three days during the winter months (defined here as November to March). Data were accessed through the U.S. Environmental Protection Agency Air Quality Database<sup>61</sup>. Averaged ALW associated with inorganic components ( $W_{\text{inorg}}$ ) was calculated using the ISORROPIAv2.1 aerosol thermodynamic equilibrium model (<http://isorroopia.eas.gatech.edu>, 2018)<sup>62</sup>. Concentrations of aerosol inorganic composition ( $\text{Na}^+$ ,  $\text{NH}_4^+$ ,  $\text{K}^+$ ,  $\text{SO}_4^{2-}$ ,  $\text{Mg}^{2+}$ ,  $\text{Ca}^{2+}$ ,  $\text{NO}_3^-$  and  $\text{Cl}^-$ ), temperature, and RH were used as model inputs. The liquid water associated with OA ( $W_{\text{org}}$ ) was calculated according to Petters and Kreidenweis (2007)<sup>63</sup> using OA concentrations as inputs with an assumed kappa value of 0.126<sup>64</sup>. The total ALW concentration was calculated as the sum of the inorganic water ( $W_{\text{inorg}}$ ) and organic water ( $W_{\text{org}}$ ) content based upon the five years (2011 to 2015) of observations, corresponding to 174 aerosol samples available for these years. The spatial distribution of aerosols in the Baltimore area is regional in nature, characterized by similar concentrations over scales of tens of kilometers<sup>65-66</sup>. This is further supported by strong correlations between OA concentrations measured at Essex and HU-Beltsville, two sites approximately equal distances from the UMBC site, over a two-year period ( $R^2 = 0.60$ , Fig. S1). Therefore, the ALW derived from the measurements at HU-Beltsville are likely representative of those at the UMBC site where the WSOC measurements were conducted.

## 2.4 CO measurements

Carbon monoxide (CO) concentrations were measured using a CO analyzer (Thermo Scientific Model 48C), with 10-min averaging during the study period. Calibration of the CO analyzer was performed prior to the sampling season. Blank measurements were obtained throughout the study and were used to determine the LOD for the CO data, which was calculated as 18 ppb<sub>v</sub>. The normalized WSOC<sub>p</sub> concentrations against CO were previously used to provide insight into the production of WSOC<sub>p</sub> mass, given that CO is considered a conservative compound relative to WSOC<sub>p</sub> and can help characterize similar processes for different airmass origins and boundary layer conditions<sup>51,67</sup>. This is a common method used to quantify SOA mass in aircraft studies, as well<sup>2,4,68-69</sup>. In our case, the background levels for WSOC<sub>p</sub> and CO were estimated as the 10<sup>th</sup> percentile for both measurements and calculated as 0.05  $\mu\text{g m}^{-3}$  and 0.15 ppm, respectively.

## 2.5 OCEC measurements

Aerosol organic carbon (OC) and elemental carbon (EC) measurements were carried out using a Sunset Labs OCEC Field Analyzer. The OCEC Analyzer was placed downstream of a PM<sub>2.5</sub> cyclone (BGI Instruments) and a parallel plate carbon denuder. The OCEC Analyzer sampled at 8 L min<sup>-1</sup> in semi-continuous mode, with 30 min sample collection followed by 15 min of off-line sample analysis according to NIOSH method 5040. The OCEC runs an external methane standard with each sample. Blank measurements were obtained once every day at midnight and were used to determine the LOD for OC and EC, which were 0.5 and 0.05  $\mu\text{g-C m}^{-3}$ , respectively<sup>70</sup>. The uncertainty of the OC and EC concentrations were  $\pm 0.2$  and 0.1  $\mu\text{g-C m}^{-3}$ , respectively. The OCEC analyzer produced a measurement every 45 minutes, compared to 14 min for WSOC. Therefore, the WSOC data were averaged to the OCEC times when comparisons between the two instruments were made. In addition, the OCEC analyzer was offline during 6 to 10 March 2015 for instrument maintenance.

### 3 Results and Discussion

#### 3.1 Study Overview

Table 1 presents an overview of measured chemical and meteorological parameters during the study. Generally, WSOC<sub>g</sub> concentrations were higher than in other seasons in Baltimore<sup>18,20</sup>, with a median value of 10.6 μg-C m<sup>-3</sup> (Table 1). Table 1 shows that the WSOC<sub>p</sub>/OC fraction was quite high (average of ~0.85), likely due to the abundance of secondary species and an overall decreasing contribution of primary OA emissions from motor vehicles<sup>71</sup>. As for the meteorological data, RH and temperature concentrations spanned a wide range capturing dry to very moist and below to above freezing conditions, respectively. Water-soluble organic carbon in the gas (WSOC<sub>g</sub>) and particle (WSOC<sub>p</sub>) phases are considered good surrogates for secondary organic gases and particles, respectively<sup>2,14,47,72</sup>. Further analyses were carried out by segregating the data into daytime (08:00 to 18:00, local time) and nighttime (20:00 to 07:00, local time) periods and based on temperature (< 0 °C, 0 – 10 °C and > 10 °C). These results are discussed below.

**Table 1.** Summary statistics of wintertime ambient measurements in Baltimore. All concentrations are reported in μg-C m<sup>-3</sup> unless otherwise noted.

Winter measurements	median	mean	standard deviation	range
WSOC <sub>g</sub>	10.6	12.5	6.8	1.6 – 42.6
WSOC <sub>p</sub>	1.8	1.9	1.0	0.1 – 6.6
WSOC <sub>p,dry</sub>	1.8	1.9	1.0	0.1 – 6.7
CO*	0.32	0.35	0.12	0.13 – 0.87
OC	1.9	2.2	0.4	0.4 – 7.5
EC	0.3	0.4	0.3	0.1 – 1.9
Relative Humidity (%)	48.0	51.9	18.1	21.0 – 91.0
Temperature (°C)	1.1	2.8	6.5	-15.9 – 20.1

\*Concentration of CO in ppm<sub>v</sub>

#### 3.2 Primary and Secondary sources of WSOC<sub>p</sub>

In this study, we use the WSOC<sub>p</sub> measurement to provide insight into the formation of OA. Previous studies have provided evidence that WSOC<sub>p</sub> is a good surrogate for SOA in many environments<sup>2,9,14</sup>, with typically minor contributions from primary sources<sup>73-74</sup>. However, under significant biomass burning influence, this assumption does not necessarily hold<sup>49</sup>, since WSOC<sub>p</sub> is also emitted directly from biomass combustion<sup>75-77</sup>.

We evaluated the assumption of WSOC<sub>p</sub> as a surrogate for SOA during the wintertime. First, we applied the EC-tracer method to estimate the abundances of primary and secondary organic aerosol mass during the wintertime in Baltimore<sup>78</sup>. The results of this analysis (Fig. S2) show that, on average, the concentration of SOA was approximately a factor of two higher than primary organic aerosol during the sampling period (67.9% ±19.1 and 32.3% ±17.7%, respectively) suggesting that WSOC<sub>p</sub> was predominantly secondary in nature.

Correlations between  $\text{WSOC}_p$  and two commonly used primary emission markers, CO and EC, also suggest that  $\text{WSOC}_p$  was a reasonable surrogate for SOA throughout much of the study. Under the three defined temperature intervals,  $\text{WSOC}_p$  was correlated with EC and CO only when temperatures were  $< 0\text{ }^\circ\text{C}$  ( $R^2 = 0.44$  and  $0.59$ , respectively, Figs S3a and S4a). For the temperature range  $0 - 10\text{ }^\circ\text{C}$ , very weak correlations were observed between  $\text{WSOC}_p$  and either EC or CO ( $R^2$  values of  $0.11$  and  $0.09$ , respectively; Figs. S3b and S4b). There was no correlation for temperatures  $> 10\text{ }^\circ\text{C}$  (Figs. S3c and S4c). This suggests an important primary component of  $\text{WSOC}_p$  only under the coldest conditions. This is supported by the diurnal profiles of  $\text{WSOC}_g$  and  $\text{WSOC}_p$  (Fig. S5), which were inconsistent with the diurnal profiles of CO and EC (Fig. S6). Note that EC and CO were highly correlated in all three temperature intervals (Fig. S7), suggesting motor vehicles as their major source<sup>79</sup>.

While these analyses do not preclude the contribution of primary  $\text{WSOC}_p$  during our study, these results collectively suggest that the majority of measured  $\text{WSOC}_p$  was secondary in nature. This finding is supported by observations in other parts of the eastern U.S., where more than half ( $\sim 60\%$ ) of the OA mass was found to be secondary during the winter<sup>25</sup>.

### 3.3 $\text{WSOC}_p$ formation through absorptive partitioning to OA

The formation of  $\text{WSOC}_p$  is first investigated through the relationship between the partitioning coefficient ( $F_p$ ) and OC concentrations (Fig. 1). The partitioning coefficient is the fraction of WSOC in the particle phase ( $F_p = \text{WSOC}_p / (\text{WSOC}_g + \text{WSOC}_p)$ ). An increase in  $F_p$  with OC suggests that WSOC partitioning was dependent on the amount of pre-existing OA and is inferred as secondary organic mass formed through gas-phase processes and absorptive uptake to the bulk OA<sup>15,50,80</sup>. Across our entire study, mean and median  $F_p$  levels increased with increasing OC concentrations, a relationship that was statistically significant at the 95% confidence level. A similar  $F_p$  dependence on OC was previously observed in Los Angeles<sup>15,51</sup>, where photochemical oxidation and absorptive partitioning contributes prominently to OA formation<sup>52,81</sup>. We note that the  $F_p$ -OC relationship was observed during the daytime and nighttime in Baltimore (Fig. S8). Note that the remaining 3 hours were considered transitional between daytime and nighttime conditions and were thus excluded from these analyses. Daytime and nighttime meteorological data are provided in the supplemental information (Table S1).

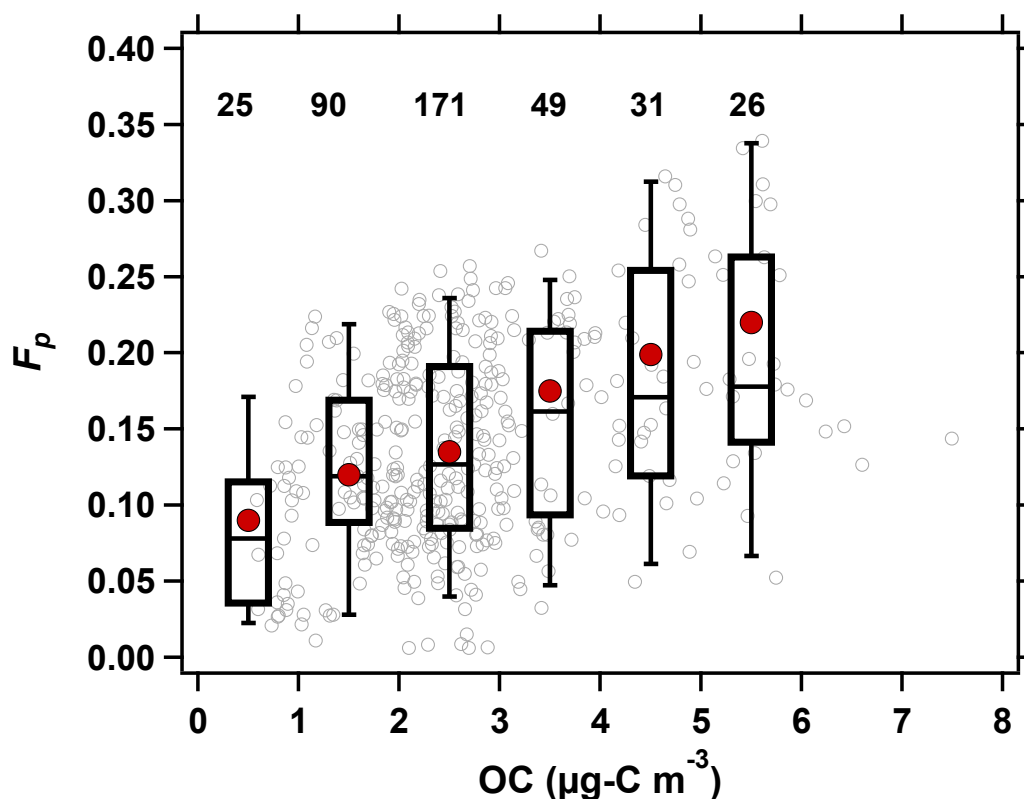


**Figure 1.** Scatter and box plots of the hourly particulate WSOC fraction,  $F_p$ , as a function of OC. Data were binned based on OC concentrations. For each bin, mean (red circles), median values (horizontal line), quartiles, as well as 5<sup>th</sup> and 95<sup>th</sup> percentiles (vertical lines) are shown. Numbers at the top represent the number of observations within each bin.

### 3.4 WSOC<sub>p</sub> formation through aqueous processes

ALW is essential for facilitating the formation of secondary WSOC<sub>p</sub> in deliquesced particles. During winter, the climatology of ALW in Baltimore shows a clear temperature dependence (Fig. 2). Typical wintertime ALW concentrations in Baltimore, including those in 2015 data, are consistently low when the temperature is below 0 °C (average ALW = 0.4 μg m<sup>-3</sup>). The level of ALW increases (> 1 μg m<sup>-3</sup>) at temperatures above 0 °C, until it reaches a maximum value (> 8 μg m<sup>-3</sup>) at temperatures above 15 °C. On freezing days (defined with average daily temperatures < 0 °C), the atmosphere was cleaner with an average PM<sub>2.5</sub> mass concentration of 10.9 ± 2.9 μg m<sup>-3</sup> compared to 15.3 ± 3.5 μg m<sup>-3</sup> on days with average daily temperatures > 0 °C. In addition, on days with average daily temperatures < 0 °C, the atmosphere was drier, with average RH levels < 40% compared to average RH levels > 65% on days where temperatures > 0 °C. This observation was likely due to the association of the lowest temperatures with air masses from Canada and/or the arctic (Fig. S9). Temperature dependence of the daily PM<sub>2.5</sub> concentrations corresponding to the same months between 2011 – 2015 are shown in Fig. S10.

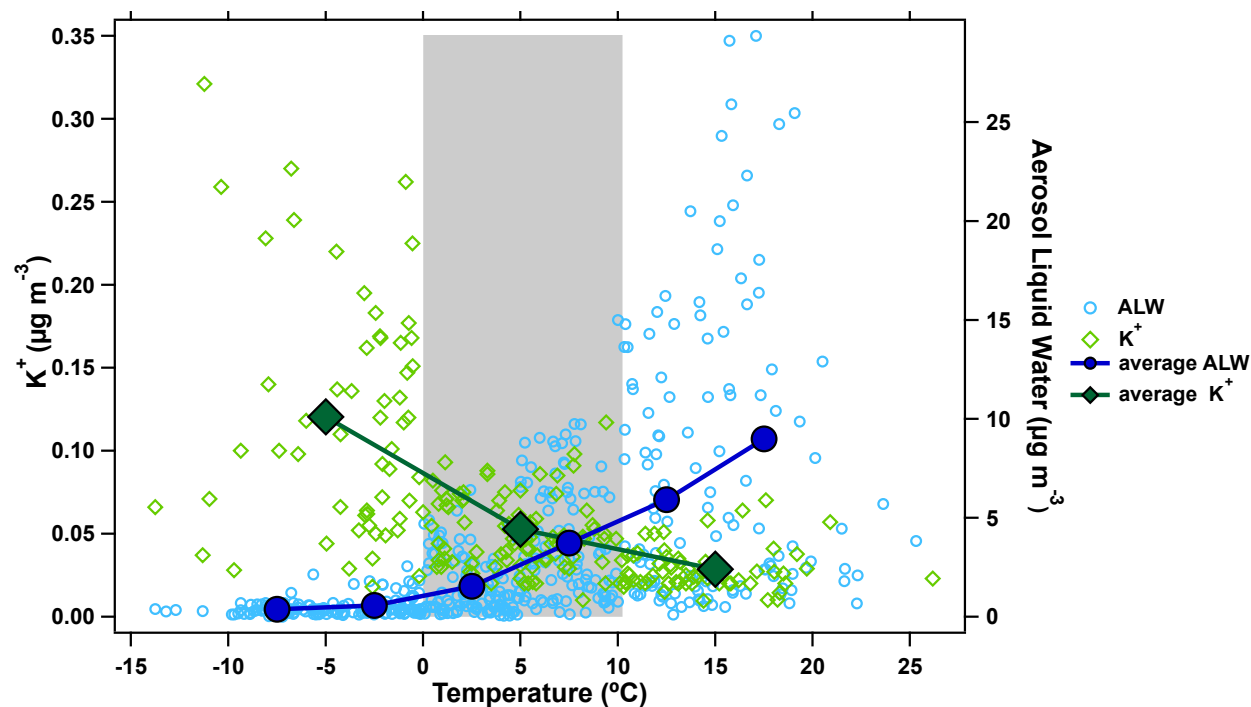


**Figure 2.** Scatterplot of aerosol potassium concentrations ( $K^+$ , green diamonds) and ALW (blue circles) as a function of temperature during the months of November through March in Baltimore over 2011 – 2015. The gray shaded area is representative of the temperature range where aqueous processing of  $WSOC_p$  was observed.

The impact of aqueous processes on secondary OA formation has previously been inferred based on an enhancement in  $F_p$  with increasing RH<sup>17-18,51,55</sup>; and is due to the uptake of  $WSOC_g$  to ALW<sup>17,82</sup>. When the wintertime data were segregated into daytime and nighttime periods, the formation of  $WSOC_p$  through aqueous processes was initially not observed since there was no enhancement in  $F_p$  as a function of RH in either period (Fig. S11). However, because the wintertime ALW content showed a strong relationship with temperature (Fig. 2), the nighttime  $WSOC_p$  data were further segregated based on temperature ( $< 0$  °C,  $0 - 10$  °C and  $> 10$  °C) as shown in Fig. 3. At night, an enhancement in  $F_p$  was observed with increasing RH for temperatures between 0 and 10 °C (Fig. 3b), suggesting the formation of  $WSOC_p$  in the aqueous phase in this temperature range. For temperatures  $< 0$  °C and  $> 10$  °C, there was no relationship between  $F_p$  and the RH (Figs. 3a and 3c, respectively), suggesting that aqueous  $WSOC_p$  was not substantially formed under such conditions. Approximately 60% of our nighttime observations were within the  $0 - 10$  °C temperature range: thus, the enhancement in  $F_p$  shows an important role of multi-phase chemistry in the formation of  $WSOC_p$  during winter. Note that such dependence on temperature was not observed for the daytime data (Fig. S12).

Aqueous processing likely contributed to secondary  $WSOC_p$  during the night rather than the daytime due to higher nighttime RH (median daytime and nighttime RH were 45% and 60%, respectively, Table S1) and hence, higher ALW. Average nighttime ALW concentrations across the entire study were more than three times higher ( $2.0 \mu\text{g m}^{-3}$ ) than during the day ( $0.6 \mu\text{g m}^{-3}$ ), consistent with ALW patterns in summer and with those determined in prior studies<sup>83</sup>. Figure S13 shows two case studies demonstrating the increase in  $F_p$  as a function of RH only at temperatures between  $0 - 10$  °C. The nighttime relationship between  $F_p$  and RH

observed was previously observed in the summer<sup>18,20</sup> and fall<sup>55</sup> in Baltimore, as well. These results show that aqueous processes can affect aerosol concentrations in the eastern U.S. throughout all seasons.

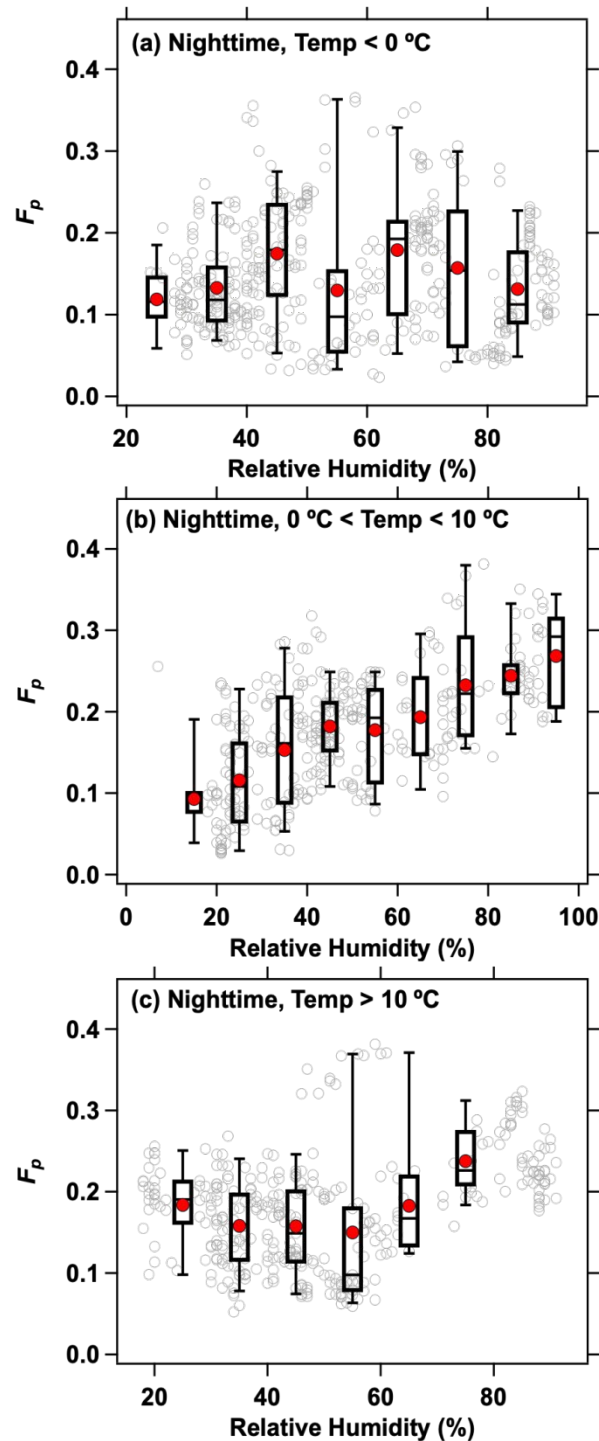


**Figure 3.** Scatter and box plots of the particulate WSOC fraction,  $F_p$ , as a function of RH at night (20:00 to 07:00, local time) for different temperature ranges: (a) < 0 °C (b) 0 – 10 °C, and (c) >10 °C. For each bin, mean (red circles, median (horizontal line), quartiles (lower and upper box values), as well as 5<sup>th</sup> and 95<sup>th</sup> percentiles (vertical lines) are shown.

The apparent conditional formation of aqueous WSOC<sub>p</sub> in the 0 – 10 °C temperature interval is further analyzed through the  $\Delta\text{WSOC}_p/\Delta\text{CO}$  ratio (Fig. 4). This ratio was used to quantify the production of WSOC<sub>p</sub> mass against the conservative atmospheric compound, CO with background levels of 0.05  $\mu\text{g m}^{-3}$  and 0.15 ppm, respectively. The  $\Delta\text{WSOC}_p/\Delta\text{CO}$  analysis shows a strong WSOC<sub>p</sub> enhancement when temperatures were between 0 – 10 °C compared to conditions when temperatures were < 0 °C or > 10 °C. Together, the results shown in Figs. 3 and 4 suggest that aqueous processes made a major contribution to the enhanced  $\Delta\text{WSOC}_p/\Delta\text{CO}$  in the 0 – 10 °C temperature interval. This is also evident by the lack of a consistent pattern in the diurnal profiles of  $\Delta\text{WSOC}_p/\Delta\text{CO}$  at temperatures < 0 °C and > 10 °C (Fig. S14). In the 0 – 10 °C temperature interval, a pronounced  $\Delta\text{WSOC}_p/\Delta\text{CO}$  enhancement was observed in the middle of the day (between 11:00 AM and 3:00 PM, local time) and at night (between 8:00 PM and 1:00 am, local time). The  $\Delta\text{WSOC}_p/\Delta\text{CO}$  enhancement during the day, when no relationship was observed between  $F_p$  and RH, suggests influence of photochemical processes and absorptive partitioning to OA, as shown in Fig. 1. On the other hand, the enhancement of  $\Delta\text{WSOC}_p/\Delta\text{CO}$  at night suggests the uptake of WSOC<sub>g</sub> to ALW, supported by Fig. 3b.

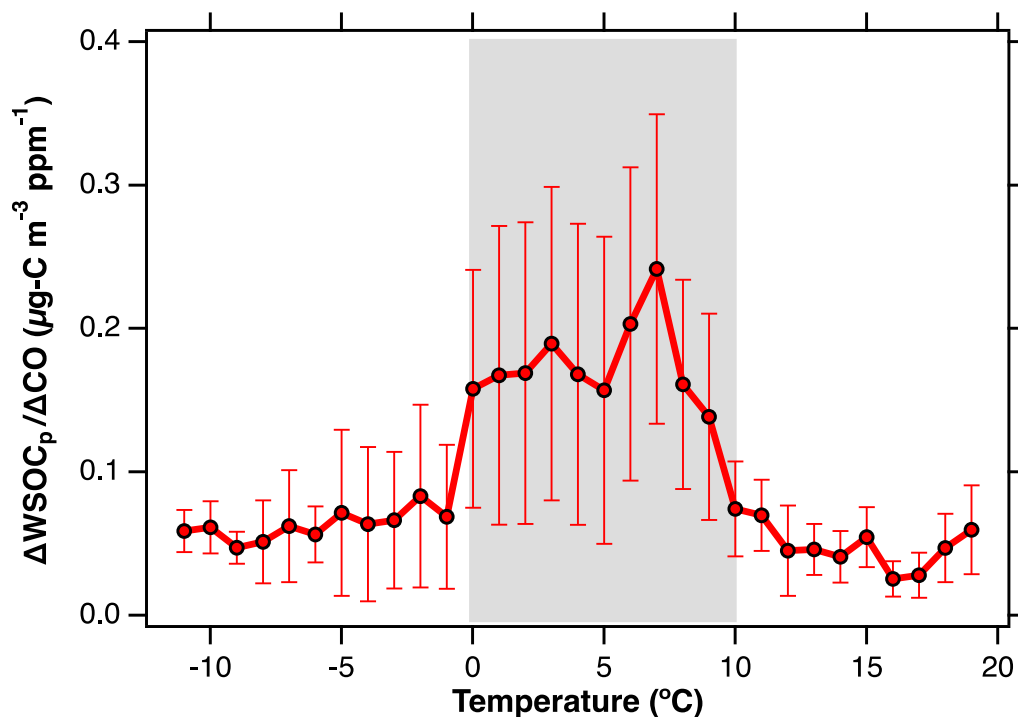


**Figure 4.** Mean  $\Delta\text{WSOC}_p/\Delta\text{CO}$  as a function of temperature. Error bars represent  $\pm$  one standard deviation. The gray shaded area shows the temperature range where aqueous processing of WSOC<sub>p</sub> was observed.

Collectively, our results suggest that secondary WSOC<sub>p</sub> formation from gas-phase oxidation and absorptive partitioning occurred consistently throughout the winter, but that aqueous WSOC<sub>p</sub> formation took place only during the night.

### 3.5 Effect of drying on $WSOC_p$

We have previously shown that there was no statistically-significant difference in the concentrations of  $WSOC_p$  and  $WSOC_{p,dry}$  for the entire wintertime data set (see Figs. 1 and S1 in El-Sayed et al.<sup>20</sup>). A detailed comparison of the  $WSOC_p$  and  $WSOC_{p,dry}$  concentrations for daytime and nighttime periods throughout the winter is shown in Fig. S15, as well. A  $WSOC_{p,dry}/WSOC_p$  ratio of unity implies that the  $WSOC_p$  did not evaporate with drying, including any  $WSOC_p$  that formed through partitioning to the OA as well<sup>20</sup>. These results indicate that ALW evaporation did not impart any effect on  $WSOC_p$  throughout the winter. This is supported by Fig. S16, which shows no change in the  $WSOC_{p,dry}/WSOC_p$  ratio as a function of RH.

However, due to the above temperature analysis that shows aqueous  $WSOC_p$  formation in the 0 – 10 °C temperature range (at night), we also applied the  $WSOC_{p,dry}/WSOC_p$  ratio analysis to the same temperature and temporal conditions. Figure 5 shows a comparison of the  $WSOC_p$  and  $WSOC_{p,dry}$  concentrations for nighttime periods in the winter for the three defined temperature intervals. Under all three conditions, the slopes were close to unity and the intercepts were close to zero, indicating the strong similarity in the  $WSOC_p$  and  $WSOC_{p,dry}$  concentrations at all temperatures. This indicates that the  $WSOC_g$  compounds that were taken up in aerosol water, causing the enhancement in  $F_p$  (Fig. 3), remained in the condensed phase upon drying. It should also be noted that our measurements indicate no effect of drying on any of the OA components we measured during the winter season. This includes no effects of particle drying on the primary component of  $WSOC_p$  that is emitted directly into the atmosphere, or the secondary portion formed through absorptive and/or aqueous partitioning in the atmosphere.

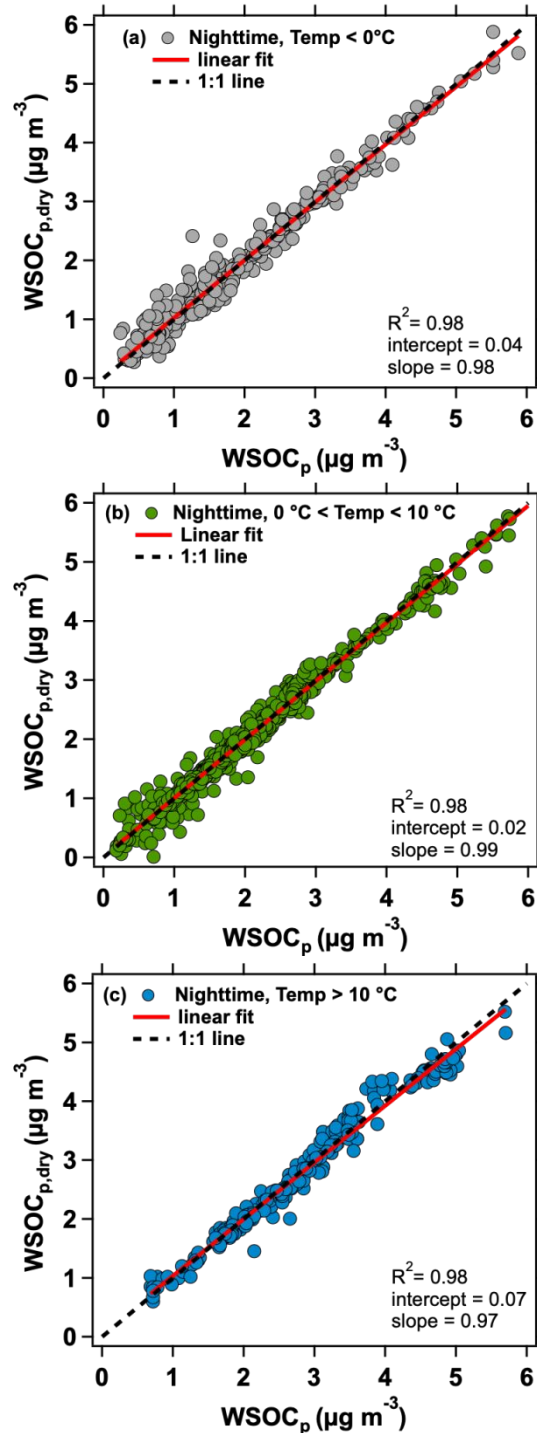


**Figure 5.** Scatter plots of  $WSOC_{p,dry}$  versus  $WSOC_p$  for nighttime periods under different temperature conditions: (a) < 0 °C (b) 0 – 10 °C, and (c) >10 °C. The solid red lines represent the linear fits to the data using least squares regression analysis; the fit parameters are given in each panel. The 1:1 line (black dashed line) is given for visual reference.

### 3.6 WSOC<sub>g</sub> and anthropogenic emissions

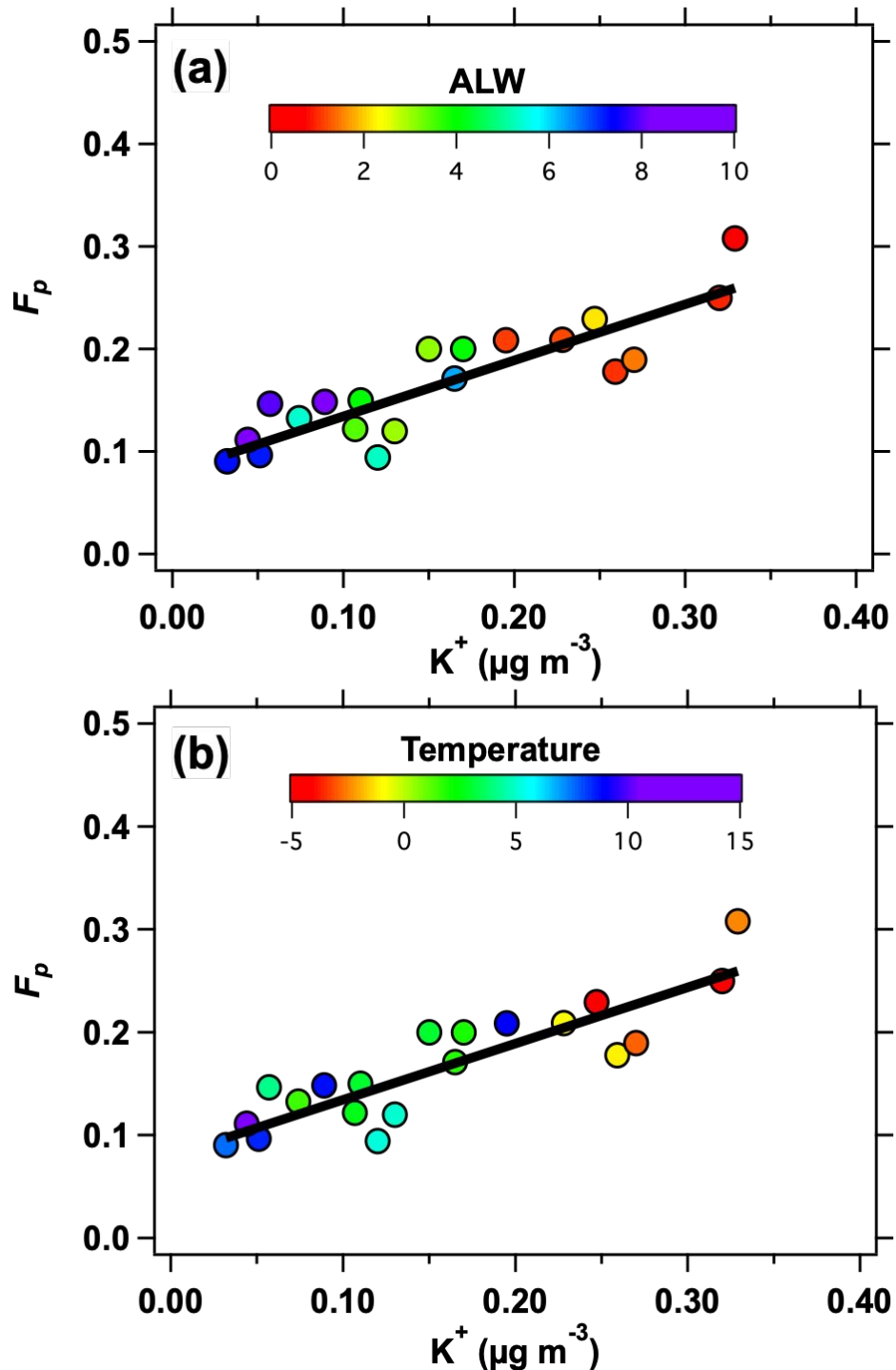
Biomass burning is a significant contributor to primary and secondary WSOC<sub>p</sub> concentrations in the winter in the eastern U.S.<sup>25</sup>. Aerosol potassium (K<sup>+</sup>) is frequently used as an indicator of biomass burning<sup>84-87</sup>. However, several studies have reported that residential biomass burning from a fireplace produces much higher potassium emissions during flaming combustion compared to emissions from wildfires or prescribed burning in which smoldering processes are more dominant<sup>88-91</sup>. Potassium emission factors are also variable depending on the fuel type<sup>92</sup>. Therefore, using potassium as a biomass burning marker may underestimate smoldering combustion emissions and emissions from certain biomass fuels. The background concentration of K<sup>+</sup> (0.015 μg m<sup>-3</sup>) in Baltimore was defined as the 10<sup>th</sup> percentile K<sup>+</sup> concentration during winter for 2011 – 2015. Average daily concentrations of WSOC<sub>g</sub> and K<sup>+</sup> were correlated (R<sup>2</sup> = 0.61, Fig. S17b) during our study, suggesting that local emissions from residential wood combustion contributed to WSOC<sub>g</sub> levels. On the other hand, daily WSOC<sub>p</sub> and K<sup>+</sup> concentrations showed no correlation (R<sup>2</sup> = 0.007, Fig. S17a). For the 0 – 10 °C temperature range, the average K<sup>+</sup> concentration (~0.06 μg m<sup>-3</sup>) was a factor of four higher than the background wintertime concentration (Fig. 3), suggesting that biomass burning was still occurring in the same temperature range where aqueous secondary aerosol formation was identified. This is emphasized since no correlations were observed between WSOC<sub>g</sub> and the vehicular tracers CO (R<sup>2</sup> = 0.06) and EC (R<sup>2</sup> = 0.10) (Figs. S18b and S19b, respectively) in this temperature range.

Scatter and boxplots of WSOC<sub>g</sub> and WSOC<sub>p</sub> concentrations as a function of wind speed (Figs. S20a and S20b, respectively) support local formation and/or direct emissions of these compounds during the winter. WSOC<sub>g</sub> and WSOC<sub>p</sub> concentrations decrease dramatically at higher wind speeds. The highest concentrations of WSOC<sub>g</sub> and WSOC<sub>p</sub> were associated with wind speeds below 2 m s<sup>-1</sup>, suggesting that the direct emission and formation of these water-soluble organic compounds were primarily taking place locally rather than being transported from elsewhere. This result is consistent with recent work conducted in the northeastern U.S. – including Maryland – suggesting a significant contribution of biomass burning emissions from residential heating towards secondary OA levels in the winter<sup>25</sup>. These observations suggest that biomass burning emissions associated with residential heating contributed significantly to the gaseous precursors which were subsequently taken up into either OA or ALW to form secondary WSOC<sub>p</sub>.

### 3.7 Factors affecting aqueous WSOC<sub>p</sub>

Enhancements in  $F_p$  with increasing RH were observed in the 0 – 10 °C temperature range (Fig. 3b), the same temperature range where both ALW concentrations (~5.0 μg m<sup>-3</sup>) and the biomass burning marker K<sup>+</sup> were also elevated (Fig. 2). At temperatures less than 0 °C, despite the abundance in biomass burning emissions, there was insufficient ALW (< 1 μg m<sup>-3</sup>) to facilitate aqueous WSOC<sub>p</sub> formation. On the other hand, at temperatures greater than 10 °C, there was an abundance of ALW (~12.0 μg m<sup>-3</sup>), but the low K<sup>+</sup> concentrations (~0.02 μg m<sup>-3</sup>) indicate minor contributions from residential biomass burning. Conditions for aqueous WSOC<sub>p</sub> formation occurred when ALW and sufficient biomass burning emissions were both present. In Baltimore, such conditions occur at night when the temperature is ~0 – 10 °C. Figures 6a and 6b depict the

24-hr averages of  $F_p$  as a function of  $K^+$  colored by ALW and temperature, respectively. Figure 6 shows that the 24-hr averages of  $F_p$  and  $K^+$  are correlated ( $R^2 = 0.77$ ), suggesting a strong relationship between the partitioning of gases into the particle phase and biomass burning emissions. This includes both gas- and aqueous-phase partitioning. The dependence of this relationship on ALW content and temperature is evident and shows that WSOC partitioning towards the particle phase enhances with  $K^+$  concentrations as ALW concentrations and temperatures decrease.



1  
2  
3 **Figure 6.** Daily averages of the partitioning coefficient  $F_p$  as a function of potassium  
4 concentrations color-coded based on (a) ALW concentrations and (b) temperature. Gray area  
5 represents the range of  $K^+$  concentrations between 0 – 10 °C where aqueous WSOC<sub>p</sub> formation is  
6 observed.  
7

8  
9 The winter results underscore the combined importance of water-soluble precursors as well  
10 as ALW for the formation of aqueous WSOC<sub>p</sub> during cold seasons. Our results highlight the  
11 importance of biomass burning emissions as precursors for aqueous WSOC<sub>p</sub> mass. In the winter  
12 and in the temperature range (0 < T < 10 °C), aqueous WSOC<sub>p</sub> formation in the Mid-Atlantic  
13 U.S. is associated with biomass burning precursors as well as ALW.  
14

15 Numerous studies carried out in other locations support our current findings, as well.  
16 Evidence of aqueous secondary OA formation from wood burning was reported in Italy in both  
17 rural and urban areas<sup>41</sup>. In Fresno, CA, evidence for aqueous secondary OA formation during  
18 the winter has previously been observed<sup>93</sup>. In Los Angeles, CA, nighttime aqueous secondary  
19 OA formation was suggested based on an increase in secondary OA at higher RH levels, possibly  
20 due to the dissolution of water-soluble primary emissions from biomass burning<sup>39</sup>. In Beijing,  
21 aqueous secondary OA formation from primary emissions – including biomass burning –  
22 contributes to episodes of high aerosol concentrations during winter<sup>41</sup>. In Paris, a modeling  
23 study showed that there was an underestimation of oxygenated organic aerosol (OOA) in winter,  
24 likely due to secondary OA formation through aqueous processing of biomass burning  
25 emissions<sup>37</sup>. In northern France, higher concentrations of the biomass burning mass  
26 spectrometry factor were associated with low wind speeds and were correlated with RH, which  
27 was attributed to aqueous processing of primary emissions to form secondary OA<sup>38</sup>. In India,  
28 aqueous processing of secondary OA was interpreted in fogs due to correlations between  
29 particulate mass and aerosol water and was suggested to be from biomass burning based on  
30 relationships between the biomass burning mass spectrometry factor and OOA<sup>94</sup>.  
31  
32

33 The ambient observations at diverse locations are supported by laboratory studies that show  
34 biomass burning is a likely source of aqueous secondary OA, as well. Phenolic compounds are  
35 emitted in high abundances from biomass burning<sup>95</sup>. Laboratory studies suggest that phenols  
36 represent a key class of aqueous secondary OA precursors, as they are highly soluble and can  
37 form lower-volatility products through an array of aqueous reactions<sup>31,35</sup>. Laboratory  
38 experiments sampling “whole” biomass burning emissions also report significant potential for  
39 aqueous secondary OA formation in cloud conditions<sup>24</sup>.  
40  
41

## 42 **4 Conclusions**

43

44 In the eastern U.S., aqueous WSOC<sub>p</sub> was observed during the winter under conditions when  
45 biomass burning emissions and sufficient ALW were both present. Our results underscore the  
46 important role of aerosol water in the formation of OA, even in the winter. These results suggest  
47 that the emissions from residential wood combustion contribute to aqueous WSOC<sub>p</sub> formation.  
48 Our results in the eastern U.S. add to the growing body of work indicating the importance of  
49 aqueous processing in the formation of organic mass from biomass burning emissions. This  
50 process is expected to contribute to OA levels in areas with high biomass burning and relatively  
51 high ALW concentrations, regardless of season. Although wood combustion for residential  
52 heating was the major form of biomass burning during this study, the results presented herein  
53 likely have implications beyond residential wood burning. Most other types of biomass burning,  
54  
55  
56  
57  
58  
59  
60

1  
2  
3 such prescribed burns, burning agricultural crop residue and wildfires, emit WSOC<sub>g</sub> that can  
4 form secondary species in the aqueous phase<sup>24,96-97</sup>. Therefore, aqueous-phase processing of  
5 biomass burning emissions in clouds and deliquescent particles is likely a widespread  
6 phenomenon that has importance for local and regional air quality as well as global climate.  
7 However, the magnitude of OA formed from this process remains highly uncertain given that  
8 unspciated compounds represent such a high fraction of gaseous emissions from biomass  
9 burning<sup>98-99</sup>. Future studies are warranted to characterize the gaseous compounds emitted from  
10 different types of biomass burning in order to evaluate their impact on OA formation.  
11  
12

### 13 **Acknowledgments**

14  
15  
16 All data used in this study have been published and are freely available (Hennigan and El-Sayed,  
17 2018). This work was supported by the National Science Foundation through Award CHE-  
18 1454763. The authors acknowledge Dr. Jose L. Jimenez for useful discussions.  
19

### 20 **References**

- 21  
22 1. Carlton AG, Turpin BJ. Particle partitioning potential of organic compounds is highest in the  
23 Eastern US and driven by anthropogenic water. *Atmospheric Chemistry and Physics*. 2013 Oct  
24 17;13(20):10203-14.  
25  
26
- 27  
28 2. Weber RJ, Sullivan AP, Peltier RE, Russell A, Yan B, Zheng M, De Gouw J, Warneke C, Brock C,  
29 Holloway JS, Atlas EL. A study of secondary organic aerosol formation in the  
30 anthropogenic-influenced southeastern United States. *Journal of Geophysical Research:*  
31 *Atmospheres*. 2007 Jul 16;112(D13).  
32  
33
- 34  
35 3. Sun YL, Zhang Q, Schwab JJ, Demerjian KL, Chen WN, Bae MS, Hung HM, Hogrefe O, Frank B,  
36 Rattigan OV, Lin YC. Characterization of the sources and processes of organic and inorganic  
37 aerosols in New York city with a high-resolution time-of-flight aerosol mass spectrometer.  
38 *Atmospheric Chemistry and Physics*. 2011 Feb 18;11(4):1581-602.  
39  
40
- 41  
42 4. Sullivan AP, Peltier RE, Brock CA, De Gouw JA, Holloway JS, Warneke C, Wollny AG, Weber  
43 RJ. Airborne measurements of carbonaceous aerosol soluble in water over northeastern United  
44 States: Method development and an investigation into water-soluble organic carbon sources.  
45 *Journal of Geophysical Research: Atmospheres*. 2006 Dec 16;111(D23).  
46  
47
- 48  
49 5. Sareen N, Moussa SG, McNeill VF. Photochemical aging of light-absorbing secondary organic  
50 aerosol material. *The Journal of Physical Chemistry A*. 2013 Apr 11;117(14):2987-96.  
51  
52  
53  
54  
55  
56  
57  
58  
59  
60

- 1  
2  
3 6. Engelhart GJ, Asa-Awuku A, Nenes A, Pandis SN. CCN activity and droplet growth kinetics of  
4 fresh and aged monoterpene secondary organic aerosol. *Atmospheric Chemistry and Physics*.  
5 2008 Jul 24;8(14):3937-49.  
6  
7
- 8  
9 7. Liu J, Bergin M, Guo H, King L, Kotra N, Edgerton E, Weber RJ. Size-resolved measurements of  
10 brown carbon in water and methanol extracts and estimates of their contribution to ambient fine-  
11 particle light absorption. *Atmospheric Chemistry and Physics*. 2013 Dec 19;13(24):12389-404.  
12  
13
- 14  
15 8. Verma V, Fang T, Guo H, King L, Bates JT, Peltier RE, Edgerton E, Russell AG, Weber RJ.  
16 Reactive oxygen species associated with water-soluble PM<sub>2.5</sub> in the southeastern United States:  
17 spatiotemporal trends and source apportionment. *Atmospheric Chemistry and Physics*. 2014 Dec  
18 8;14(23):12915-30.  
19  
20  
21
- 22  
23 9. Timonen H, Carbone S, Aurela M, Saarnio K, Saarikoski S, Ng NL, Canagaratna MR, Kulmala M,  
24 Kerminen VM, Worsnop DR, Hillamo R. Characteristics, sources and water-solubility of ambient  
25 submicron organic aerosol in springtime in Helsinki, Finland. *Journal of aerosol science*. 2013  
26 Feb 1;56:61-77.  
27  
28  
29
- 30  
31 10. Duong HT, Sorooshian A, Craven JS, Hersey SP, Metcalf AR, Zhang X, Weber RJ, Jonsson H,  
32 Flagan RC, Seinfeld JH. Water-soluble organic aerosol in the Los Angeles Basin and outflow  
33 regions: Airborne and ground measurements during the 2010 CalNex field campaign. *Journal of*  
34 *Geophysical Research: Atmospheres*. 2011 Nov 16;116(D21).  
35  
36  
37
- 38  
39 11. Timonen H, Aurela M, Carbone S, Saarnio K, Saarikoski S, Mäkelä T, Kulmala M, Kerminen VM,  
40 Worsnop DR, Hillamo R. High time-resolution chemical characterization of the water-soluble  
41 fraction of ambient aerosols with PILS-TOC-IC and AMS. *Atmospheric Measurement Techniques*.  
42 2010 Aug 18;3(4):1063-74.  
43  
44  
45
- 46  
47 12. Graham B, Mayol-Bracero OL, Guyon P, Roberts GC, Decesari S, Facchini MC, Artaxo P,  
48 Maenhaut W, Köll P, Andreae MO. Water-soluble organic compounds in biomass burning  
49 aerosols over Amazonia 1. Characterization by NMR and GC-MS. *Journal of Geophysical*  
50 *Research: Atmospheres*. 2002 Oct 27;107(D20):LBA-14.  
51  
52  
53  
54  
55  
56  
57

- 1  
2  
3 13. Mayol-Bracero OL, Guyon P, Graham B, Roberts G, Andreae MO, Decesari S, Facchini MC,  
4 Fuzzi S, Artaxo P. Water-soluble organic compounds in biomass burning aerosols over Amazonia  
5  
6 2. Apportionment of the chemical composition and importance of the polyacidic fraction. *Journal*  
7  
8 *of Geophysical Research: Atmospheres*. 2002 Oct 27;107(D20):LBA-59.  
9
- 10  
11 14. Kondo Y, Miyazaki Y, Takegawa N, Miyakawa T, Weber RJ, Jimenez JL, Zhang Q, Worsnop DR.  
12  
13 Oxygenated and water-soluble organic aerosols in Tokyo. *Journal of Geophysical Research:*  
14  
15 *Atmospheres*. 2007 Jan 16;112(D1).  
16
- 17 15. Zhang X, Liu Z, Hecobian A, Zheng M, Frank NH, Edgerton ES, Weber RJ. Spatial and seasonal  
18  
19 variations of fine particle water-soluble organic carbon (WSOC) over the southeastern United  
20  
21 States: implications for secondary organic aerosol formation. *Atmospheric Chemistry and*  
22  
23 *Physics*. 2012 Jul 25;12(14):6593-607.  
24
- 25 16. Asa-Awuku A, Nenes A, Gao S, Flagan RC, Seinfeld JH. Water-soluble SOA from Alkene  
26  
27 ozonolysis: composition and droplet activation kinetics inferences from analysis of CCN activity.  
28  
29 *Atmospheric Chemistry and Physics*. 2010 Feb 15;10(4):1585-97.  
30
- 31 17. Hennigan CJ, Bergin MH, Dibb JE, Weber RJ. Enhanced secondary organic aerosol formation  
32  
33 due to water uptake by fine particles. *Geophysical Research Letters*. 2008 Sep;35(18).  
34
- 35 18. El-Sayed MMH, Amenumey D, Hennigan CJ. Drying-induced evaporation of secondary organic  
36  
37 aerosol during summer. *Environmental Science & Technology*. 2016 Apr 5;50(7):3626-33.  
38
- 39 19. McNeill VF. Aqueous organic chemistry in the atmosphere: Sources and chemical processing of  
40  
41 organic aerosols. 2015 Jan 22;49(3):1237-1244.  
42
- 43 20. El-Sayed MMH, Ortiz-Montalvo DL, Hennigan CJ. The effects of isoprene and NO<sub>x</sub> on secondary  
44  
45 organic aerosols formed through reversible and irreversible uptake to aerosol water. *Atmospheric*  
46  
47 *Chemistry and Physics*. 2018 Jan 30;18(2):1171-84.  
48
- 49 21. Li X, Han J, Hopke PK, Hu J, Shu Q, Chang Q, Ying Q. Quantifying primary and secondary  
50  
51 humic-like substances in urban aerosol based on emission source characterization and a source-  
52  
53 oriented air quality model. *Atmospheric Chemistry and Physics*. 2019 Feb 22;19(4):2327-41.  
54  
55  
56  
57  
58  
59  
60

- 1  
2  
3 22. Szidat S, Prévôt AS, Sandradewi J, Alfarra MR, Synal HA, Wacker L, Baltensperger U. Dominant  
4 impact of residential wood burning on particulate matter in Alpine valleys during winter.  
5 Geophysical Research Letters. 2007 Mar;34(5).  
6  
7  
8  
9 23. Du Z, He K, Cheng Y, Duan F, Ma Y, Liu J, Zhang X, Zheng M, Weber R. A yearlong study of  
10 water-soluble organic carbon in Beijing I: Sources and its primary vs. secondary nature.  
11 Atmospheric Environment. 2014 Aug 1;92:514-21.  
12  
13  
14  
15 24. Tomaz S, Cui T, Chen Y, Sexton KG, Roberts JM, Warneke C, Yokelson RJ, Surratt JD, Turpin  
16 BJ. Photochemical cloud processing of primary wildfire emissions as a potential source of  
17 secondary organic aerosol. Environmental science & technology. 2018 Aug 28;52(19):11027-37.  
18  
19  
20  
21 25. Schroder JC, Campuzano-Jost P, Day DA, Shah V, Larson K, Sommers JM, Sullivan AP,  
22 Campos T, Reeves JM, Hills A, Hornbrook RS. Sources and secondary production of organic  
23 aerosols in the northeastern United States during WINTER. Journal of Geophysical Research:  
24 Atmospheres. 2018 Jul 27;123(14):7771-96.  
25  
26  
27  
28  
29 26. Grieshop AP, Donahue NM, Robinson AL. Laboratory investigation of photochemical oxidation of  
30 organic aerosol from wood fires 2: analysis of aerosol mass spectrometer data. Atmospheric  
31 Chemistry and Physics. 2009 Mar 27;9(6):2227-40.  
32  
33  
34  
35 27. Grieshop AP, Logue JM, Donahue NM, Robinson AL. Laboratory investigation of photochemical  
36 oxidation of organic aerosol from wood fires 1: measurement and simulation of organic aerosol  
37 evolution. Atmospheric Chemistry and Physics. 2009 Feb 18;9(4):1263-77.  
38  
39  
40  
41 28. Robinson AL, Donahue NM, Shrivastava MK, Weitkamp EA, Sage AM, Grieshop AP, Lane TE,  
42 Pierce JR, Pandis SN. Rethinking organic aerosols: Semivolatile emissions and photochemical  
43 aging. Science. 2007 Mar 2;315(5816):1259-62.  
44  
45  
46  
47 29. Hennigan CJ, Miracolo MA, Engelhart GJ, May AA, Presto AA, Lee T, Sullivan AP, McMeeking  
48 GR, Coe H, Wold CE, Hao WM. Chemical and physical transformations of organic aerosol from  
49 the photo-oxidation of open biomass burning emissions in an environmental chamber.  
50 Atmospheric Chemistry and Physics. 2011 Aug 1;11(15):7669-86.  
51  
52  
53  
54  
55  
56  
57  
58  
59  
60

- 1  
2  
3 30. Anastasio C, Faust BC, Rao CJ. Aromatic carbonyl compounds as aqueous-phase  
4 photochemical sources of hydrogen peroxide in acidic sulfate aerosols, fogs, and clouds. 1. Non-  
5 phenolic methoxybenzaldehydes and methoxyacetophenones with reductants (phenols).  
6 Environmental science & technology. 1996 Dec 30;31(1):218-32.  
7  
8  
9  
10  
11 31. Yu L, Smith J, Laskin A, George KM, Anastasio C, Laskin J, Dillner AM, Zhang Q. Molecular  
12 transformations of phenolic SOA during photochemical aging in the aqueous phase: competition  
13 among oligomerization, functionalization, and fragmentation. Atmospheric Chemistry and  
14 Physics. 2016 Apr 13;16(7):4511-27.  
15  
16  
17  
18  
19 32. Smith JD, Kinney H, Anastasio C. Phenolic carbonyls undergo rapid aqueous photodegradation  
20 to form low-volatility, light-absorbing products. Atmospheric Environment. 2016 Feb 1;126:36-44.  
21  
22  
23 33. Huang DD, Zhang Q, Cheung HH, Yu L, Zhou S, Anastasio C, Smith JD, Chan CK. Formation  
24 and evolution of aqSOA from aqueous-phase reactions of phenolic carbonyls: Comparison  
25 between ammonium sulfate and ammonium nitrate solutions. Environmental science &  
26 technology. 2018 Jul 9;52(16):9215-24.  
27  
28  
29  
30  
31 34. Smith JD, Sio V, Yu L, Zhang Q, Anastasio C. Secondary organic aerosol production from  
32 aqueous reactions of atmospheric phenols with an organic triplet excited state. Environmental  
33 science & technology. 2014 Jan 21;48(2):1049-57.  
34  
35  
36  
37 35. Yu L, Smith J, Laskin A, Anastasio C, Laskin J, Zhang Q. Chemical characterization of SOA  
38 formed from aqueous-phase reactions of phenols with the triplet excited state of carbonyl and  
39 hydroxyl radical. Atmospheric Chemistry and Physics. 2014 Dec 23;14(24):13801-16.  
40  
41  
42  
43 36. Ge X, Setyan A, Sun Y, Zhang Q. Primary and secondary organic aerosols in Fresno, California  
44 during wintertime: Results from high resolution aerosol mass spectrometry. Journal of  
45 Geophysical Research: Atmospheres. 2012 Oct 16;117(D19).  
46  
47  
48  
49 37. Fountoukis C, Megaritis AG, Skyllakou K, Charalampidis PE, Denier van der Gon HA, Crippa M,  
50 Prévôt AS, Fachinger F, Wiedensohler A, Pilinis C, Pandis SN. Simulating the formation of  
51 carbonaceous aerosol in a European Megacity (Paris) during the MEGAPOLI summer and winter  
52 campaigns. Atmospheric Chemistry and Physics. 2016 Mar 21;16(6):3727-41.  
53  
54  
55  
56  
57  
58  
59  
60

- 1  
2  
3 38. Rodelas RR, Chakraborty A, Perdrix E, Tison E, Riffault V. Real-time assessment of wintertime  
4 organic aerosol characteristics and sources at a suburban site in northern France. *Atmospheric*  
5 *Environment*. 2019 Apr 15;203:48-61.  
6  
7  
8  
9 39. Saffari A, Hasheminassab S, Shafer MM, Schauer JJ, Chatila TA, Sioutas C. Nighttime aqueous-  
10 phase secondary organic aerosols in Los Angeles and its implication for fine particulate matter  
11 composition and oxidative potential. *Atmospheric environment*. 2016 May 1;133:112-22.  
12  
13  
14 40. Gilardoni S, Massoli P, Paglione M, Giulianelli L, Carbone C, Rinaldi M, Decesari S, Sandrini S,  
15 Costabile F, Gobbi GP, Pietrogrande MC. Direct observation of aqueous secondary organic  
16 aerosol from biomass-burning emissions. *Proceedings of the National Academy of Sciences*.  
17 2016 Sep 6;113(36):10013-8.  
18  
19  
20 41. Hu W, Hu M, Hu W, Jimenez JL, Yuan B, Chen W, Wang M, Wu Y, Chen C, Wang Z, Peng J.  
21 Chemical composition, sources, and aging process of submicron aerosols in Beijing: Contrast  
22 between summer and winter. *Journal of Geophysical Research: Atmospheres*. 2016 Feb  
23 27;121(4):1955-77.  
24  
25  
26 42. Kuang Y, He Y, Xu W, Yuan B, Zhang G, Ma Z, Wu C, Wang C, Wang S, Zhang S, Tao J.  
27 Photochemical aqueous-phase reactions induce rapid daytime formation of oxygenated organic  
28 aerosol on the North China Plain. *Environmental Science & Technology*. 2020 Mar 4;54(7):3849-  
29 60.  
30  
31  
32 43. Wang Y, Wang Q, Ye J, Li L, Zhou J, Ran W, Zhang R, Wu Y, Cao J. Chemical composition and  
33 sources of submicron aerosols in winter at a regional site in Beijing-Tianjin-Hebei region:  
34 Implications for the Joint Action Plan. *Science of The Total Environment*. 2020 Jun 1;719:137547.  
35  
36  
37 44. Duan J, Huang RJ, Gu Y, Lin C, Zhong H, Xu W, Liu Q, You Y, Ovadnevaite J, Ceburnis D,  
38 Hoffmann T. Measurement report: Large contribution of biomass burning and aqueous-phase  
39 processes to the wintertime secondary organic aerosol formation in Xi'an, Northwest China.  
40 *Atmospheric Chemistry and Physics Discussions*. 2022 Mar 3:1-20.  
41  
42  
43 45. Porter WC, Jimenez JL, Barsanti KC. Quantifying atmospheric parameter ranges for ambient  
44 secondary organic aerosol formation. *ACS Earth and Space Chemistry*. 2021 Jul 14;5(9):2380-  
45 97.  
46  
47  
48  
49  
50  
51  
52  
53  
54  
55  
56  
57  
58  
59  
60

- 1  
2  
3  
4 46. Shah V, Jaeglé L, Jimenez JL, Schroder JC, Campuzano-Jost P, Campos TL, Reeves JM, Stell  
5 M, Brown SS, Lee BH, Lopez-Hilfiker FD. Widespread pollution from secondary sources of  
6 organic aerosols during winter in the Northeastern United States. *Geophysical Research Letters*.  
7 2019 Mar 16;46(5):2974-83.  
8  
9  
10  
11 47. Hennigan CJ, Bergin MH, Russell AG, Nenes A, Weber RJ. Gas/particle partitioning of water-  
12 soluble organic aerosol in Atlanta. *Atmospheric Chemistry and Physics*. 2009 Jun 4;9(11):3613-  
13 28.  
14  
15  
16  
17 48. Sareen N, Carlton AG, Surratt JD, Gold A, Lee B, Lopez-Hilfiker FD, Mohr C, Thornton JA, Zhang  
18 Z, Lim YB, Turpin BJ. Identifying precursors and aqueous organic aerosol formation pathways  
19 during the SOAS campaign. *Atmospheric Chemistry and Physics*. 2016 Nov 21;16(22):14409-20.  
20  
21  
22  
23 49. Youn JS, Wang Z, Wonaschütz A, Arellano A, Betterton EA, Sorooshian A. Evidence of aqueous  
24 secondary organic aerosol formation from biogenic emissions in the North American Sonoran  
25 Desert. *Geophysical research letters*. 2013 Jul 16;40(13):3468-72.  
26  
27  
28  
29 50. Xu L, Guo H, Weber RJ, Ng NL. Chemical characterization of water-soluble organic aerosol in  
30 contrasting rural and urban environments in the southeastern United States. *Environmental*  
31 *Science & Technology*. 2017 Jan 3;51(1):78-88.  
32  
33  
34  
35 51. Zhang X, Liu J, Parker ET, Hayes PL, Jimenez JL, de Gouw JA, Flynn JH, Grossberg N, Lefer  
36 BL, Weber RJ. On the gas-particle partitioning of soluble organic aerosol in two urban  
37 atmospheres with contrasting emissions: 1. Bulk water-soluble organic carbon. *Journal of*  
38 *Geophysical Research: Atmospheres*. 2012 Nov 16;117(D21).  
39  
40  
41  
42 52. Zhang X, Lin YH, Surratt JD, Zotter P, Prévôt AS, Weber RJ. Light-absorbing soluble organic  
43 aerosol in Los Angeles and Atlanta: A contrast in secondary organic aerosol. *Geophysical*  
44 *Research Letters*. 2011 Nov;38(21).  
45  
46  
47  
48 53. Yan C, Zheng M, Sullivan AP, Shen G, Chen Y, Wang S, Zhao B, Cai S, Desyaterik Y, Li X, Zhou  
49 T. Residential coal combustion as a source of levoglucosan in China. *Environmental science &*  
50 *technology*. 2018 Feb 6;52(3):1665-74.  
51  
52  
53  
54  
55  
56  
57  
58  
59  
60

- 1  
2  
3 54. Ondov JM, Buckley TJ, Hopke PK, Ogulei D, Parlange MB, Rogge WF, Squibb KS, Johnston MV,  
4 Wexler AS. Baltimore Supersite: Highly time-and size-resolved concentrations of urban PM<sub>2.5</sub> and  
5 its constituents for resolution of sources and immune responses. *Atmospheric Environment*. 2006  
6 Jan 1;40:224-37.  
7  
8  
9  
10  
11 55. El-Sayed MMH, Wang Y, Hennigan CJ. Direct atmospheric evidence for the irreversible formation  
12 of aqueous secondary organic aerosol. *Geophysical Research Letters*. 2015 Jul 16;42(13):5577-  
13 86.  
14  
15  
16  
17 56. Hennigan CJ, El-Sayed MMH, Hodzic A. Detailed characterization of a mist chamber for the  
18 collection of water-soluble organic gases. *Atmospheric environment*. 2018 Sep 1;188:12-7.  
19  
20  
21 57. Orsini DA, Ma Y, Sullivan A, Sierau B, Baumann K, Weber RJ. Refinements to the particle-into-  
22 liquid sampler (PILS) for ground and airborne measurements of water-soluble aerosol  
23 composition. *Atmospheric Environment*. 2003 Mar 1;37(9-10):1243-59.  
24  
25  
26  
27 58. Sullivan AP, Weber RJ, Clements AL, Turner JR, Bae MS, Schauer JJ. A method for on-line  
28 measurement of water-soluble organic carbon in ambient aerosol particles: Results from an urban  
29 site. *Geophysical Research Letters*. 2004 Jul;31(13).  
30  
31  
32  
33 59. Hinds WC. *Aerosol technology: properties, behavior, and measurement of airborne particles*.  
34 John Wiley & Sons; 1999 Jan 19.  
35  
36  
37 60. Hennigan CJ, El-Sayed MMH. Atmospheric water-soluble organic carbon in Baltimore, MD,  
38 Knowledge Network for Biocomplexity.2018.  
39  
40  
41 61. EPA, <https://aqs.epa.gov/api>, 2018.  
42  
43 62. Fountoukis C, Nenes A. ISORROPIA II: a computationally efficient thermodynamic equilibrium  
44 model for K<sup>+</sup>-Ca<sup>2+</sup>-Mg<sup>2+</sup>-NH<sub>4</sub><sup>+</sup>-Na<sup>+</sup>-SO<sub>4</sub><sup>2-</sup>-NO<sub>3</sub><sup>-</sup>-Cl<sup>-</sup>-H<sub>2</sub>O aerosols. *Atmospheric Chemistry and*  
45 *Physics*. 2007 Sep 13;7(17):4639-59.  
46  
47  
48 63. Petters MD, Kreidenweis SM. A single parameter representation of hygroscopic growth and cloud  
49 condensation nucleus activity. *Atmospheric Chemistry and Physics*. 2007 Apr 18;7(8):1961-71.  
50  
51  
52  
53  
54  
55  
56  
57  
58  
59  
60

- 1  
2  
3 64. Guo H, Xu L, Bougiatioti A, Cerully KM, Capps SL, Hite Jr JR, Carlton AG, Lee SH, Bergin MH,  
4 Ng NL, Nenes A. Fine-particle water and pH in the southeastern United States. *Atmospheric*  
5 *Chemistry and Physics*. 2015 May 11;15(9):5211-28.  
6  
7  
8  
9 65. Beyersdorf AJ, Ziemba LD, Chen G, Corr CA, Crawford JH, Diskin GS, Moore RH, Thornhill KL,  
10 Winstead EL, Anderson BE. The impacts of aerosol loading, composition, and water uptake on  
11 aerosol extinction variability in the Baltimore–Washington, DC region. *Atmospheric Chemistry and*  
12 *Physics*. 2016 Jan 28;16(2):1003-15.  
13  
14  
15  
16 66. Chu DA, Ferrare R, Szykman J, Lewis J, Scarino A, Hains J, Burton S, Chen G, Tsai T, Hostetler  
17 C, Hair J. Regional characteristics of the relationship between columnar AOD and surface PM<sub>2.5</sub>:  
18 Application of lidar aerosol extinction profiles over Baltimore–Washington Corridor during  
19 DISCOVER-AQ. *Atmospheric Environment*. 2015 Jan 1;101:338-49.  
20  
21  
22  
23  
24 67. de Gouw J, Jimenez JL. Organic aerosols in the Earth's atmosphere. 2009 Sept 16; 43(20):  
25 7614–7618.  
26  
27  
28  
29 68. May AA, Lee T, McMeeking GR, Akagi S, Sullivan AP, Urbanski S, Yokelson RJ, Kreidenweis  
30 SM. Observations and analysis of organic aerosol evolution in some prescribed fire smoke  
31 plumes. *Atmospheric Chemistry and Physics*. 2015 Jun 11;15(11):6323-35.  
32  
33  
34  
35 69. de Gouw JA, Brock CA, Atlas EL, Bates TS, Fehsenfeld FC, Goldan PD, Holloway JS, Kuster  
36 WC, Lerner BM, Matthew BM, Middlebrook AM. Sources of particulate matter in the northeastern  
37 United States in summer: 1. Direct emissions and secondary formation of organic matter in urban  
38 plumes. *Journal of Geophysical Research: Atmospheres*. 2008 Apr 27;113(D8).  
39  
40  
41  
42 70. Valerino MJ, Johnson JJ, Izumi J, Orozco D, Hoff RM, Delgado R, Hennigan CJ. Sources and  
43 composition of PM<sub>2.5</sub> in the Colorado Front Range during the DISCOVER-AQ study. *Journal of*  
44 *Geophysical Research: Atmospheres*. 2017 Jan 16;122(1):566-82.  
45  
46  
47  
48 71. McDonald BC, Goldstein AH, Harley RA. Long-term trends in California mobile source emissions  
49 and ambient concentrations of black carbon and organic aerosol. *Environmental science &*  
50 *technology*. 2015 Apr 21;49(8):5178-88.  
51  
52  
53  
54  
55  
56  
57  
58  
59  
60

- 1  
2  
3 72. Hodzic A, Aumont B, Knote C, Lee-Taylor J, Madronich S, Tyndall G. Volatility dependence of  
4 Henry's law constants of condensable organics: Application to estimate depositional loss of  
5 secondary organic aerosols. *Geophysical Research Letters*. 2014 Jul 16;41(13):4795-804.  
6  
7  
8  
9 73. Du Z, He K, Cheng Y, Duan F, Ma Y, Liu J, Zhang X, Zheng M, Weber R. A yearlong study of  
10 water-soluble organic carbon in Beijing II: Light absorption properties. *Atmospheric Environment*.  
11 2014 Jun 1;89:235-41.  
12  
13  
14 74. Psichoudaki M, Pandis SN. Atmospheric aerosol water-soluble organic carbon measurement: a  
15 theoretical analysis. *Environmental science & technology*. 2013 Sep 3;47(17):9791-8.  
16  
17  
18 75. Zhang X, Hecobian A, Zheng M, Frank NH, Weber RJ. Biomass burning impact on PM<sub>2.5</sub> over the  
19 southeastern US during 2007: integrating chemically speciated FRM filter measurements, MODIS  
20 fire counts and PMF analysis. *Atmospheric Chemistry and Physics*. 2010 Jul 23;10(14):6839-53.  
21  
22  
23 76. Hecobian A, Zhang X, Zheng M, Frank N, Edgerton ES, Weber RJ. Water-Soluble Organic  
24 Aerosol material and the light-absorption characteristics of aqueous extracts measured over the  
25 Southeastern United States. *Atmospheric Chemistry and Physics*. 2010 Jul 2;10(13):5965-77.  
26  
27  
28 77. Cho SY, Park SS. Resolving sources of water-soluble organic carbon in fine particulate matter  
29 measured at an urban site during winter. *Environmental Science: Processes & Impacts*.  
30 2013;15(2):524-34.  
31  
32  
33 78. Cabada JC, Pandis SN, Subramanian R, Robinson AL, Polidori A, Turpin B. Estimating the  
34 secondary organic aerosol contribution to PM<sub>2.5</sub> using the EC tracer method special issue of  
35 aerosol science and technology on findings from the fine particulate matter supersites program.  
36 *Aerosol Science and Technology*. 2004 Dec 1;38(S1):140-55.  
37  
38  
39 79. Kondo Y, Komazaki Y, Miyazaki Y, Moteki N, Takegawa N, Kodama D, Deguchi S, Nogami M,  
40 Fukuda M, Miyakawa T, Morino Y. Temporal variations of elemental carbon in Tokyo. *Journal of*  
41 *Geophysical Research: Atmospheres*. 2006 Jun 27;111(D12).  
42  
43  
44 80. Donahue NM, Robinson AL, Pandis SN. Atmospheric organic particulate matter: From smoke to  
45 secondary organic aerosol. *Atmospheric Environment*. 2009 Jan 1;43(1):94-106.  
46  
47  
48  
49  
50  
51  
52  
53  
54  
55  
56  
57  
58  
59  
60

- 1  
2  
3 81. Ortega AM, Hayes PL, Peng Z, Palm BB, Hu W, Day DA, Li R, Cubison MJ, Brune WH, Graus M,  
4 Warneke C. Real-time measurements of secondary organic aerosol formation and aging from  
5 ambient air in an oxidation flow reactor in the Los Angeles area. *Atmospheric Chemistry and*  
6 *Physics*. 2016 Jun 15;16(11):7411-33.  
7  
8  
9  
10  
11 82. Hodas N, Sullivan AP, Skog K, Keutsch FN, Collett Jr JL, Decesari S, Facchini MC, Carlton AG,  
12 Laaksonen A, Turpin BJ. Aerosol liquid water driven by anthropogenic nitrate: implications for  
13 lifetimes of water-soluble organic gases and potential for secondary organic aerosol formation.  
14 *Environmental science & technology*. 2014 Oct 7;48(19):11127-36.  
15  
16  
17  
18  
19 83. Battaglia Jr MA, Douglas S, Hennigan CJ. Effect of the urban heat island on aerosol pH.  
20 *Environmental science & technology*. 2017 Nov 21;51(22):13095-103.  
21  
22  
23 84. Pachon JE, Weber RJ, Zhang X, Mulholland JA, Russell AG. Revising the use of potassium (K) in  
24 the source apportionment of PM<sub>2.5</sub>. *Atmospheric Pollution Research*. 2013 Jan 1;4(1):14-21.  
25  
26  
27 85. Ding X, He QF, Shen RQ, Yu QQ, Zhang YQ, Xin JY, Wen TX, Wang XM. Spatial and seasonal  
28 variations of isoprene secondary organic aerosol in China: Significant impact of biomass burning  
29 during winter. *Scientific reports*. 2016 Feb 4;6(1):1-0.  
30  
31  
32  
33 86. Sullivan AP, Holden AS, Patterson LA, McMeeking GR, Kreidenweis SM, Malm WC, Hao WM,  
34 Wold CE, Collett Jr JL. A method for smoke marker measurements and its potential application  
35 for determining the contribution of biomass burning from wildfires and prescribed fires to ambient  
36 PM<sub>2.5</sub> organic carbon. *Journal of Geophysical Research: Atmospheres*. 2008 Nov 27;113(D22).  
37  
38  
39  
40  
41 87. Saarikoski S, Timonen H, Saarnio K, Aurela M, Järvi L, Keronen P, Kerminen VM, Hillamo R.  
42 Sources of organic carbon in fine particulate matter in northern European urban air. *Atmospheric*  
43 *chemistry and physics*. 2008 Oct 29;8(20):6281-95.  
44  
45  
46  
47 88. Echalar F, Gaudichet A, Cachier H, Artaxo P. Aerosol emissions by tropical forest and savanna  
48 biomass burning: characteristic trace elements and fluxes. *Geophysical research letters*. 1995  
49 Nov 15;22(22):3039-42.  
50  
51  
52  
53 89. Lee T, Sullivan AP, Mack L, Jimenez JL, Kreidenweis SM, Onasch TB, Worsnop DR, Malm W,  
54 Wold CE, Hao WM, Collett Jr JL. Chemical smoke marker emissions during flaming and  
55  
56  
57  
58  
59  
60

- 1  
2  
3 smoldering phases of laboratory open burning of wildland fuels. *Aerosol Science and Technology*.  
4  
5 2010 Aug 9;44(9):i-v.  
6
- 7 90. Sullivan AP, Frank N, Onstad G, Simpson CD, Collett Jr JL. Application of high-performance  
8  
9 anion-exchange chromatography–pulsed amperometric detection for measuring carbohydrates in  
10  
11 routine daily filter samples collected by a national network: 1. Determination of the impact of  
12  
13 biomass burning in the upper Midwest. *Journal of Geophysical Research: Atmospheres*. 2011 Apr  
14  
15 27;116(D8).  
16
- 17 91. Ward TJ, Hamilton Jr RF, Dixon RW, Paulsen M, Simpson CD. Characterization and evaluation  
18  
19 of smoke tracers in PM: results from the 2003 Montana wildfire season. *Atmospheric*  
20  
21 *Environment*. 2006 Nov 1;40(36):7005-17.  
22
- 23 92. McMeeking GR, Kreidenweis SM, Baker S, Carrico CM, Chow JC, Collett Jr JL, Hao WM, Holden  
24  
25 AS, Kirchstetter TW, Malm WC, Moosmüller H. Emissions of trace gases and aerosols during the  
26  
27 open combustion of biomass in the laboratory. *Journal of Geophysical Research: Atmospheres*.  
28  
29 2009 Oct 16;114(D19).  
30
- 31 93. Sun YL, Zhang Q, Anastasio C, Sun J. Insights into secondary organic aerosol formed via  
32  
33 aqueous-phase reactions of phenolic compounds based on high resolution mass spectrometry.  
34  
35 *Atmospheric Chemistry and Physics*. 2010 May 26;10(10):4809-22.  
36
- 37 94. Chakraborty A, Bhattu D, Gupta T, Tripathi SN, Canagaratna MR. Real-time measurements of  
38  
39 ambient aerosols in a polluted Indian city: Sources, characteristics, and processing of organic  
40  
41 aerosols during foggy and nonfoggy periods. *Journal of Geophysical Research: Atmospheres*.  
42  
43 2015 Sep 16;120(17):9006-19.  
44
- 45 95. Mazzoleni LR, Zielinska B, Moosmüller H. Emissions of levoglucosan, methoxy phenols, and  
46  
47 organic acids from prescribed burns, laboratory combustion of wildland fuels, and residential  
48  
49 wood combustion. *Environmental science & technology*. 2007 Apr 1;41(7):2115-22.  
50
- 51 96. Burling IR, Yokelson RJ, Akagi SK, Urbanski SP, Wold CE, Griffith DW, Johnson TJ, Reardon J,  
52  
53 Weise DR. Airborne and ground-based measurements of the trace gases and particles emitted by  
54  
55 prescribed fires in the United States. *Atmospheric Chemistry and Physics*. 2011 Dec  
56  
57 7;11(23):12197-216.  
58  
59  
60

- 1  
2  
3 97. Kawamura K, Tachibana E, Okuzawa K, Aggarwal SG, Kanaya Y, Wang ZF. High abundances of  
4 water-soluble dicarboxylic acids, ketocarboxylic acids and  $\alpha$ -dicarbonyls in the mountaintop  
5 aerosols over the North China Plain during wheat burning season. *Atmospheric chemistry and*  
6 *physics*. 2013 Aug 22;13(16):8285-302.  
7  
8  
9  
10  
11 98. Yokelson RJ, Burling IR, Gilman JB, Warneke C, Stockwell CE, De Gouw J, Akagi SK, Urbanski  
12 SP, Veres P, Roberts JM, Kuster WC. Coupling field and laboratory measurements to estimate  
13 the emission factors of identified and unidentified trace gases for prescribed fires. *Atmospheric*  
14 *Chemistry and Physics*. 2013 Jan 7;13(1):89-116.  
15  
16  
17  
18  
19 99. Jathar SH, Gordon TD, Hennigan CJ, Pye HO, Pouliot G, Adams PJ, Donahue NM, Robinson AL.  
20 Unspeciated organic emissions from combustion sources and their influence on the secondary  
21 organic aerosol budget in the United States. *Proceedings of the National Academy of Sciences*.  
22  
23  
24  
25  
26  
27  
28  
29  
30  
31  
32  
33  
34  
35  
36  
37  
38  
39  
40  
41  
42  
43  
44  
45  
46  
47  
48  
49  
50  
51  
52  
53  
54  
55  
56  
57  
58  
59  
60